

On the rapid spectral variability of Be-stars: high spectral resolution study of γ Cas, ϕ Per, and 59 Cyg

A. Chalabaev¹ and J. P. Maillard²

¹ Laboratoire Associé au C.N.R.S. No. 325, Observatoire de Meudon, F-92195 Meudon, France

² Canada-France-Hawaii Telescope, P.O. Box 1597, Kamuela, HI 96743, USA

Received February 26, accepted June 8, 1983

Summary. An intensive search of rapid spectral variations with the time resolution from 15 s to 15 min is performed for 3 Be stars. In total, 57 spectra in H α and 8 spectra in the λ 8500 Å spectral region were obtained during 4 nights. A detailed analysis of possible instrumental effects and statistical uncertainties is made. An expression to estimate the uncertainty of the equivalent width measurements is obtained. A method to select the variations of the line profile from those induced by the continuum level instabilities is described. Results of this study show that, in general, there are no rapid variations of H α and of the lines of the λ 8500 Å region (O I λ 8446 Å, Paschen lines and the infrared triplet of Ca II). Only slow (time scale of several hours) changes in the H α profile can occur at the limit of our detection (1–2% of F_c). Slower night-to-night changes of H α are clearly detected.

Key words: Be-stars – rapid variability – variable stars – stellar spectroscopy

I. Introduction

The variability of Be-stars with time scales of years, months and days is well known (e.g., Underhill and Doazan, 1982 and references therein). The majority of studied Be stars have shown changes in brightness, color and emission line profiles. Moreover, there are many stars which can lose their emission features within several years interval and vice versa (Hubert-Delplace and Hubert, 1979; Jaschek et al., 1980). Thus, a system of a main sequence B star, surrounded by a gaseous envelope, is shown to be essentially a variable-unstable system, and studies of variability are of great importance for understanding the Be star phenomenon.

New details could come from observations with a temporal resolution as short as hours and minutes. Recent discovery of *photometric* variations with time scale of several hours for a considerable number of Be stars in *UBV*- and *uvby*-filters seems to indicate the presence of non-radial pulsations in these stars. This should be an important feature for the theoretical modelling (Lester, 1975; Percy et al., 1981; Spear et al., 1981; Percy, 1982). The situation is more doubtful for the rapid *spectral* variability. Even the question whether observed variations are really stellar

ones is considered as not yet having received an answer (see reviews by Hutchings, 1976; Slettebak, 1978, 1982; Underhill and Doazan, 1982). In fact, the majority of studies which give a negative answer on the question of reality of the rapid variations were made with a low spectral resolution and a low photometric precision (typical uncertainty of the equivalent width $\sigma(W) \approx 5\%$ for $W \approx 20$ Å); also, the total survey time for one star did not exceed 8 h (Baliunas and Guinan, 1976; Haefner et al., 1975; Lacy, 1977; Reynolds and Slettebak, 1978). Such observations cannot exclude the occurrence of small line profile variations, which do not affect considerably the equivalent width (EW) of the line. On the other hand, the works, which claim the reality of the rapid variations of the line profile (Bijaoui and Doazan, 1979; Hutchings et al., 1971; Luud, 1978; Mamatkazina, 1978; Slettebak and Snow, 1978), are based on observations made on moderate size telescopes. Consequently, high temporal and spectral resolutions were obtained by decreasing security limits relative to different kinds of noise. Those results must be considered with a caution (Hutchings, 1976; Lacy, 1977; Slettebak, 1982).

It is clear that new high spectral resolution observations, obtained on a large telescope with a high signal-to-noise ratio, and accompanied by a careful analysis of possible instrumental effects, are necessary to confirm the reality of the rapid spectral variations. In this article we present such observations of γ Cas, ϕ Per and 59 Cyg in the H α region. A limited study of the rapid variability was also performed in λ 8500 Å spectral region for γ Cas and ϕ Per. The lines of this region (Paschen lines of hydrogen, lines of the infrared triplet of Ca II and O I λ 8446 Å) are formed in different physical conditions. This fact allows an opportunity of simultaneous study of variabilities, arising in different parts of the stellar envelope, which makes the λ 8500 Å particularly interesting.

II. Observations and reduction of spectra

Observations were made by one of (J.P.M.) at the Mauna Kea Observatory with the 1872 pixels cooled Reticon detector installed at the coudé-spectrograph of the 3.6 m Canada–France–Hawaii telescope. Spectra of γ Cas and ϕ Per were obtained in 1981, November 14, 15, and 16 and those of 59 Cyg in 1982, June 6. The effective dispersion was 72 mÅ per pixel and the covered spectral interval was about 130 Å. To estimate the spectral resolution we used narrow telluric lines of H $_2$ O. We obtained a value of 0.2 Å in agreement with results by other observers (e.g., Hobbs and Campbell, 1982). Flat-field spectra of different exposure were obtained every night and stellar spectra were divided on the corresponding flat-field spectrum, which was the same for all

Send offprint requests to: A. Chalabaev

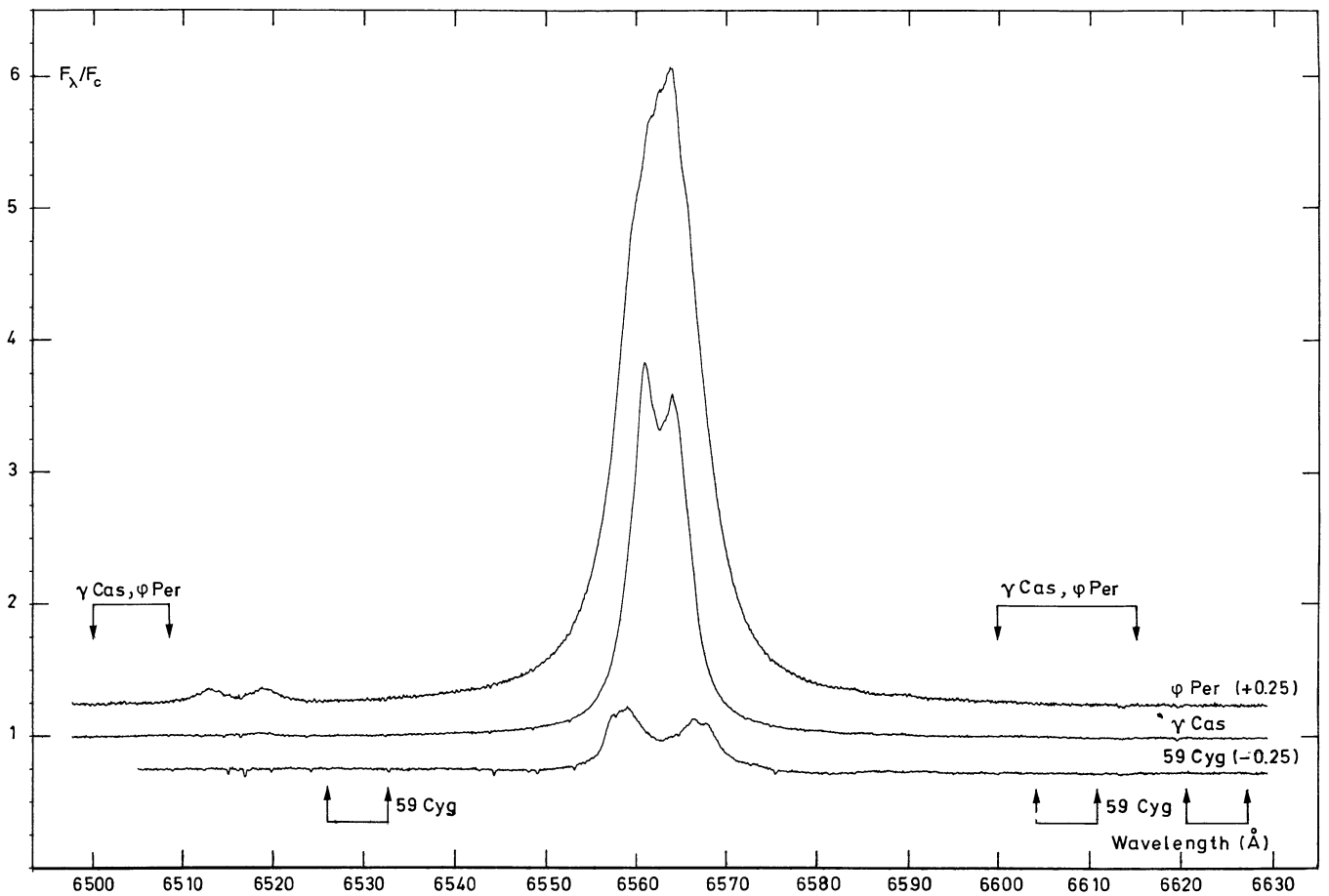


Fig. 1. Typical spectra obtained in the H_α region. Arrows indicate the location of bands used for the continuum level determination. The value of a constant added to the plot is indicated in brackets just after the star name. The presented spectra of γ Cas and ϕ Per were obtained in 1981 Nov. 15, that of 59 Cyg in 1982 June 6

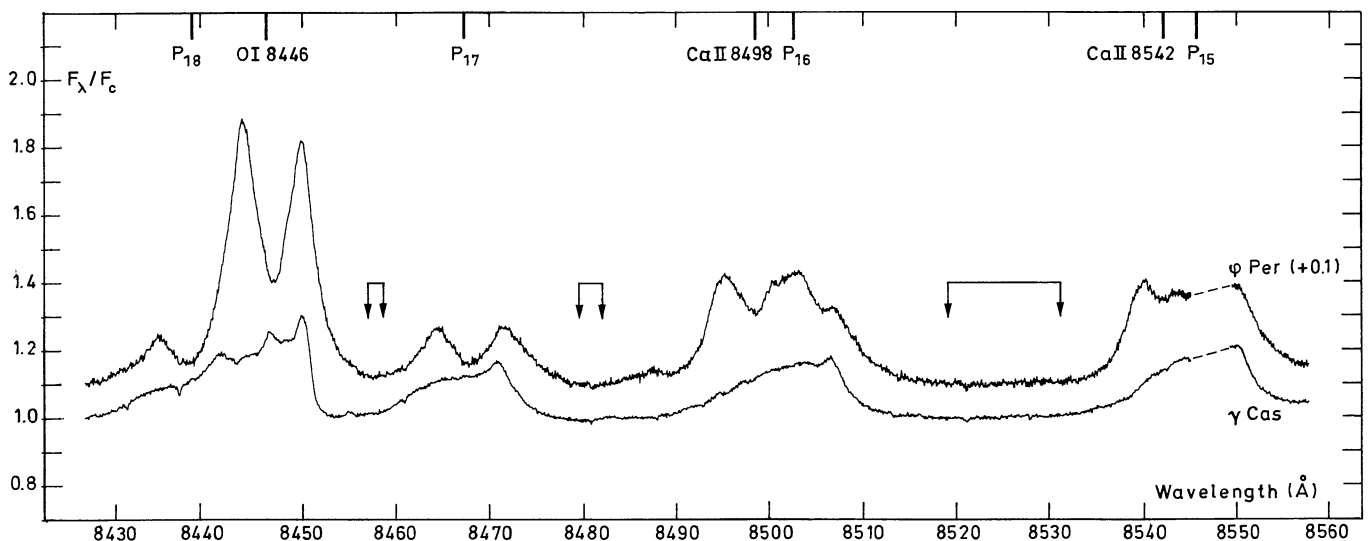


Fig. 2. Typical spectra obtained in the $\lambda 8500 \text{ \AA}$ region. Arrows indicate the location of bands used for the continuum level determination. The spectra were obtained in 1981 Nov. 16

spectra of one sequence. Since H_α in Be stars often has extended wings, which can affect the normalisation procedure (Slettebak and Reynolds, 1978; Fontaine et al., 1982), one must be careful in choosing the regions of the continuum. The spacing of 1800 km s^{-1} from the H_α line center, used by us, is believed to be necessary and sufficient. The least mean square calculations (100 pixel read-outs used) yield the value of uncertainty of the continuum level determination $\sigma(F_c)/F_c$. It was $\leq 0.15\%$ for ϕ Per, and $\leq 0.1\%$ for γ Cas and 59 Cyg in the H_α region. The real uncertainty must be somewhat higher, probably, by a factor of 2 to 3.

All reduction has been done on the VAX-11 computer of the Meudon Observatory by software, written by one of us (A.C.) especially for the search of spectral variations. Typical spectra, obtained in the H_α region, are plotted in Fig. 1 and those of the $\lambda 8500 \text{ \AA}$ region in Fig. 2. It is useful to outline that the normalised spectra are always expressed in terms of the relative flux F_λ/F_c , and not in terms of the relative intensity I_λ/I_c , as it is believed sometimes (e.g. in *Proc. IAU Symp. 70* and *98*, devoted to Be stars). The conversion into intensities is possible only when the region responsible for the line emission and that responsible for the emission in the adjacent continuum have equal solid angles, which are cancelled during the normalisation procedure. This condition is not satisfied in the case of envelope lines.

A summary of observational conditions and measured values for the H_α spectral region are given in Table 1. The first six columns present respectively star names, the date of observations, the UT of the exposure start for the first and for the last spectra of sequences, the number of spectra in a sequence and the exposure time for a single spectrum. The typical value of the signal-to noise ratio, measured in the continuum is listed in the Column (7). Values of EW for H_α and for the $\text{Fe II } \lambda 6516 \text{ \AA}$ emission with corresponding values of the measured rms deviation σ_M are given in Columns (8) and (14), respectively. The value σ_M represents the spread of EW values measured for the corresponding sequence of spectra. However, due to a residual effect of the Reticon, the EW values of H_α for the first spectra of each sequence must be excluded from the calculation of the mean value of EW and σ_M . The absolute value of EW of H_α calculated in this way, contains a systematic error which is not important for the variability studies. A more detailed discussion of the Reticon behaviour and its implications are given in Sect. III. The EW values of the $\text{Fe II } \lambda 6516 \text{ \AA}$ emission line were calculated using the continuum defined in the vicinity of the line. This emission, which is much weaker than H_α , was not affected by instrumental effects, and its EW values listed in Table 2 are correct. The EW values of H_α of 59 Cyg are also free from instrumental effects. Since we deal only with emission lines, the negative sign of EW is omitted everywhere in Tables.

Observations in the $\lambda 8500 \text{ \AA}$ spectral region are presented in Table 2. Its columns are analogous to those of Table 1. The determination of the continuum level was a problem in this region, since almost all emissions do overlap (see Fig. 2). The covered spectral interval was not sufficient to establish precisely the continuum level. Nevertheless, a comparison of our data for ϕ Per with those obtained by Polidan and Peters (1976) in the same spectral region but with a larger covered spectral interval, about 200 \AA , has shown that the systematic error introduced in the continuum level determination can be estimated not exceeding 5% . The statistical rms error provided by the least square method is $\sigma(F_c)/F_c \approx 0.3\%$. It is instructive to compare the measured values $\sigma_M(W)$ of the variation of EW to the expected error $\sigma_T(W)$ due to statistical fluctuations alone. The theoretical analysis of the uncertainties, arising during EW measurements, is made in

Table 1. Observations in the 6500–6630 \AA spectral region

Star	UT date	UT start	UT end	Number of spectra	Exposure time (s)	S/N ratio	H_α $\lambda 6563 \text{ \AA}$		$\text{Fe II } \lambda 6516 \text{ \AA}$				
							$W \pm \sigma_M^a$ (8)	σ_T (9)	F_{\max}/F_c (10)	F_{\min}/F_c (11)	V/R (12)	$\Delta\lambda_{1/2}$ (13)	$W \pm \sigma_M$ (14)
γ Cas	1981 Nov. 14	6 ^h 01	6 ^h 08	2	50	170	—	3.90 \pm 0.03	3.37 \pm 0.02	1.08 \pm 0.01	6.84 \pm 0.07	0.045 \pm 0.005	0.004
γ Cas	1981 Nov. 14	7 54	8 04	6	15	80–150	—	3.95 \pm 0.05	3.42 \pm 0.04	1.08 \pm 0.01	6.91 \pm 0.07	0.052 \pm 0.007	0.004
γ Cas	1981 Nov. 14	9 17	9 37	5	25 or 50	200	24.70 \pm 0.14	3.90 \pm 0.06	3.40 \pm 0.06	1.08 \pm 0.01	6.84 \pm 0.07	0.047 \pm 0.002	0.004
γ Cas	1981 Nov. 14	10 11	10 55	4	50	200	24.60 \pm 0.24	3.93 \pm 0.01	3.42 \pm 0.01	1.08 \pm 0.01	6.86 \pm 0.07	0.047 \pm 0.004	0.004
γ Cas	1981 Nov. 15	5 33	6 03	8	50	220	24.40 \pm 0.24	3.90 \pm 0.02	3.36 \pm 0.04	1.07 \pm 0.01	6.98 \pm 0.07	0.046 \pm 0.002	0.004
γ Cas	1981 Nov. 16	5 56	6 22	6	50 or 100	220	23.90 \pm 0.24	3.89 \pm 0.02	3.36 \pm 0.02	1.07 \pm 0.01	6.91 \pm 0.07	0.034 \pm 0.005	0.004
γ Cas	1981 Nov. 16	8 20	8 22	2	50	200	—	3.80 \pm 0.14	3.28 \pm 0.12	1.07 \pm 0.02	6.91 \pm 0.07	0.035 \pm 0.004	0.004
ϕ Per	1981 Nov. 14	8 16	9 02	8	50	60–100	—	5.96 \pm 0.10	—	—	9.32 \pm 0.07	0.68 \pm 0.04	0.03
ϕ Per	1981 Nov. 15	6 18	6 36	5	50 or 100	90–150	56.37 \pm 0.25	5.81 \pm 0.02	—	—	9.37 \pm 0.07	0.68 \pm 0.05	0.03
ϕ Per	1981 Nov. 16	6 37	6 54	5	100	90–150	57.40 \pm 0.20	6.11 \pm 0.02	—	—	9.07 \pm 0.07	0.63 \pm 0.02	0.03
59 Cyg	1982 June 6	3 35	5 50	6	1000	120	5.02 \pm 0.04	1.48 \pm 0.01	1.22 \pm 0.01	1.07 \pm 0.02	—	—	—

^a All $\Delta\lambda_{1/2}$, W , σ_M and σ_T values are given in \AA

For H_α of γ Cas the values of W contain a systematical error which remains constant during a sequence (see explanations in the text)

Table 2. Observations in the 8430–8560 Å spectral region (1981, November 16)

Star	UT 1981 Nov. 16		Number of spectra	Exposure time (s)	S/N ratio	$P_{18} + O I \lambda 8446 \text{ \AA}$		P_{17}		$P_{16} + Ca II \lambda 8498 \text{ \AA}$		$P_{15} + Ca II \lambda 8542 \text{ \AA}$	
	start	end				$W \pm \sigma_M$	σ_T	$W \pm \sigma_M$	σ_T	$W \pm \sigma_M$	σ_T	$W \pm \sigma_M$	σ_T
(1)	(2)	(3)	(4)	(5)	(6)	(7)	(8)	(9)	(10)	(11)	(12)	(13)	(14)
γ Cas	7 ^h 43	7 ^h 56	4	100 or 200	220	3.27 ± 0.03	0.02	1.55 ± 0.03	0.02	2.14 ± 0.03	0.03	2.49 ± 0.03	0.04
ϕ Per	7 ^h 02	7 ^h 28	4	100 or 400	160	7.17 ± 0.06	0.06	1.75 ± 0.07	0.09	4.82 ± 0.07	0.10	4.50 ± 0.12	0.20

Note: All W , σ_M , and σ_T values are given in Å

Appendix. In Columns (9) and (13) of Table 1 and in Columns (8), (10), (12), and (14) of Table 2 we list the values of $\sigma_T(W)$, calculated by means of expression (A8) of the Appendix. The measured uncertainty $\sigma_M(W)$ was calculated as the standard deviation of EW. Its values are in a good agreement with the theoretical estimates $\sigma_T(W)$, except those for the H_α spectra of γ Cas, obtained in November 14, 1981, UT 7:54–8:04, and for the H_α spectra of ϕ Per, obtained in the same night. Those spectral sequences show unusually high variations of EW. It was found that these variations are caused by instrumental effects. Due to a failure of the exposure-meter during this period, it was necessary to replace the image slicer, which is normally in use at the entrance of the spectrograph, by a slit. The slit height was greater than the height of Reticon pixels, and unavoidable guiding errors gave rise to variations of the slope of the continuum, and consequently, to a higher uncertainty of the continuum level. Nevertheless, those spectra can be used for the search of the rapid variations of the line profile (see next section).

III. Method of detection of spectral variations

a) Subtraction of consecutive spectra

It is easy to show that such a subtraction is more sensitive to profile variations than a similar division of spectra. Some typical differences are plotted in Fig. 3a (γ Cas, November 15) and Fig. 4a (ϕ Per, November 14). The rms noise on the difference plots measured on wavelengths corresponding to the centre of H_α was about 1% for γ Cas and about 4% for ϕ Per; the values are given relative to the corresponding continuum level. Changes of the line profile considerably higher than the noise are clearly seen. It is striking that the absolute value of the difference is roughly proportional to the relative flux F_λ/F_c at this wavelength. If we superimpose the corresponding normalized spectra, the phenomenon looks like an increase or decrease of the H_α line as a whole above the continuum level. We will show that such variations are explained by slight variations of the value adopted for the continuum level. The fact that the observed H_α lines are strongly in emission as well as the high signal-to-noise ratio amplify the continuum level effects.

Let us perform a simple mathematical analysis of the spectral variability. We can decompose the stellar flux F_λ into a sum of the continuum flux F_c and the bound-bound flux L_λ . Then, for a normalized spectrum one can write:

$$R_\lambda = \frac{F_\lambda}{F_c} = 1 + \frac{L_\lambda}{F_c}. \quad (1)$$

For the next spectrum in a sequence we will have:

$$R'_\lambda = 1 + \frac{L_\lambda + \Delta L_\lambda}{F_c + \Delta F_c}, \quad (2)$$

where ΔL_λ is the variation of the bound-bound emission, and ΔF_c is that of the continuum one F_c . If $\Delta F_c/F_c \ll 1$, then for the difference $\Delta R'_\lambda$ between two spectra one can write:

$$\Delta R'_\lambda = R'_\lambda - R_\lambda = \frac{L_\lambda}{F_c} \left(\frac{\Delta L_\lambda}{L_\lambda} - \frac{\Delta F_c}{F_c} \right). \quad (3)$$

This expression shows that if the variation contains a “gray” term, which is constant over the width of the line, this term will be modulated by the line profile function L_λ/F_c , and that is just what is seen in Fig. 3a and Fig. 4a. The “gray” term is simply the variation of the continuum level $\Delta F_c/F_c$. Surely, one can suppose that the variation of the bound-bound flux $\Delta L_\lambda/L_\lambda$ also may be constant over all wavelengths of H_α . However, the time scale of variations (2–3 min) makes such an assumption quite unlikely. In fact, different parts of the line profile are formed in different parts of an extended envelope of size $R_{\text{env}} \gtrsim 10R_*$, where R_* is the radius of the central star. For a hypothetical mechanism, changing the amount of the bound-bound spectral flux L_λ in the same proportion in all parts of the envelope, even if it travels as fast as the light, it would take at least 20 min to cross the envelope and to achieve the modification of the line profile. This time scale argument is sufficient to exclude from consideration the *rapid* variations of L_λ on a *large* wavelength scale. Variations of L_λ on a small wavelength scale, i.e. true profile variations, are possible, but on the difference plots they can be masked by the variations due to ΔF_c . Let us develop a method to separate these two kinds of variations.

b) Separation of the line profile variations

We will use the fact that the wavelengths scales of the variations are different, the profile variations being limited to small parts of the line. The method consists in suppressing the variations caused by instabilities of the continuum level. Then, the new difference plots are used for a detection of the profile variations, while the value of the applied suppression provides the measure of the continuum level instability.

Let us denote through G_λ the variable factor of the expression (2), so that

$$G_\lambda = \frac{\Delta L_\lambda}{L_\lambda} - \frac{\Delta F_c}{F_c}. \quad (4)$$

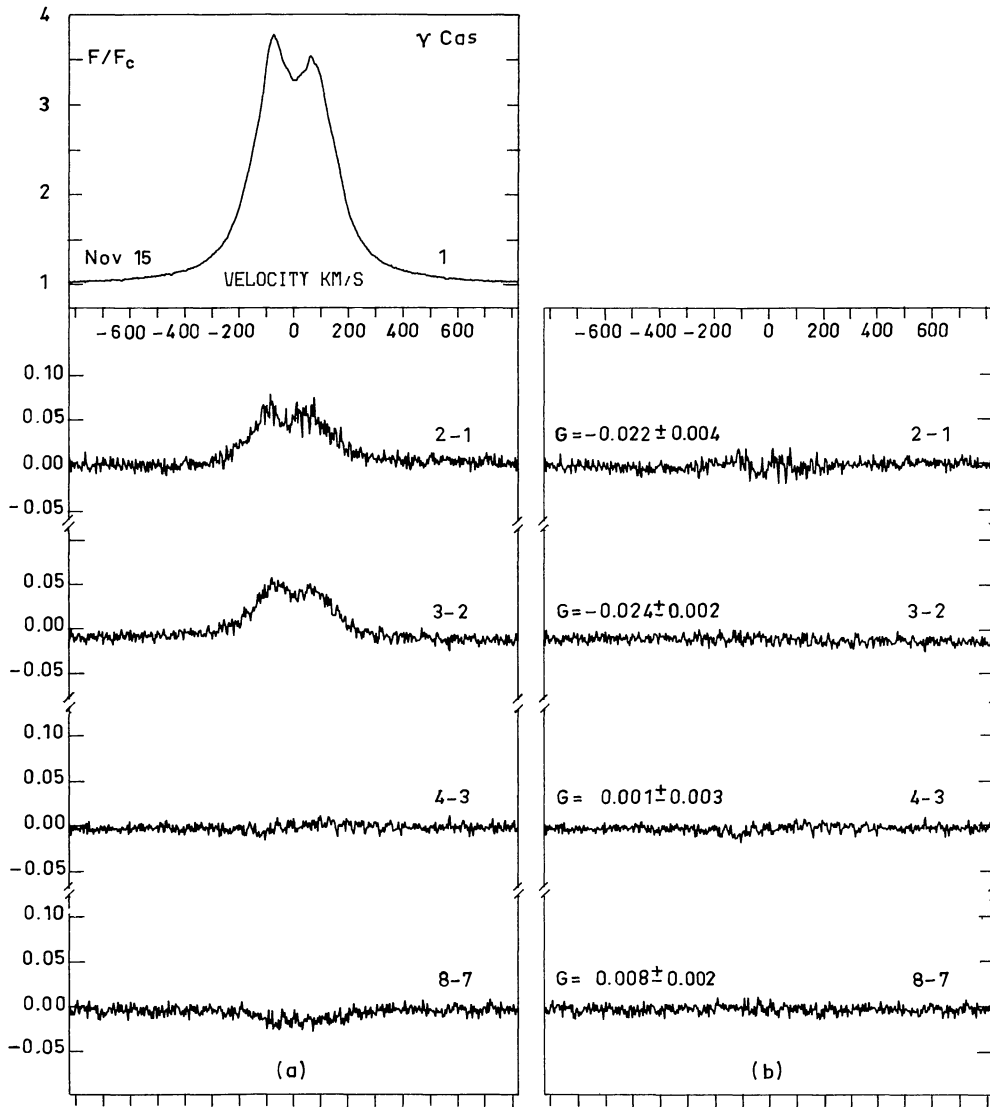


Fig. 3a and b. Search of rapid variations of H_α (γ Cas): **a** differences of consecutive spectra, **b** same difference, but the variations due to fluctuations of the continuum level are suppressed. Spectra were obtained in 1981 Nov. 15, UT's of the exposure start are as follows: 1: $5^{\text{h}}33^{\text{m}}2$, 2: $5^{\text{h}}46^{\text{m}}2$, 3: $5^{\text{h}}53^{\text{m}}6$, 4: $5^{\text{h}}55^{\text{m}}6$, ..., 7: $6^{\text{h}}01^{\text{m}}4$, 8: $6^{\text{h}}02^{\text{m}}9$

Using the expressions (1) and (3), one can relate G_λ to measurable quantities:

$$G_\lambda = \frac{\Delta R'_\lambda}{R_\lambda - 1} \quad (5)$$

that provides a mean to calculate the values G_λ . Now, if G_λ is averaged over all wavelengths of the line, the contribution of the profile variations, caused by $\Delta L_\lambda/L_\lambda$, into the mean value will be small, and we can write:

$$\bar{G} \simeq -\frac{\Delta F_c}{F_c} \quad (6)$$

Locating the wavelengths, where G_λ differs significantly from \bar{G} , one can exclude their contribution and calculate a new, more exact value of \bar{G} . A comparison of the expressions (2) and (3) shows that the suppression of the variations due to ΔF_c can be obtained, if the second spectrum in the difference couple is

corrected in the following way:

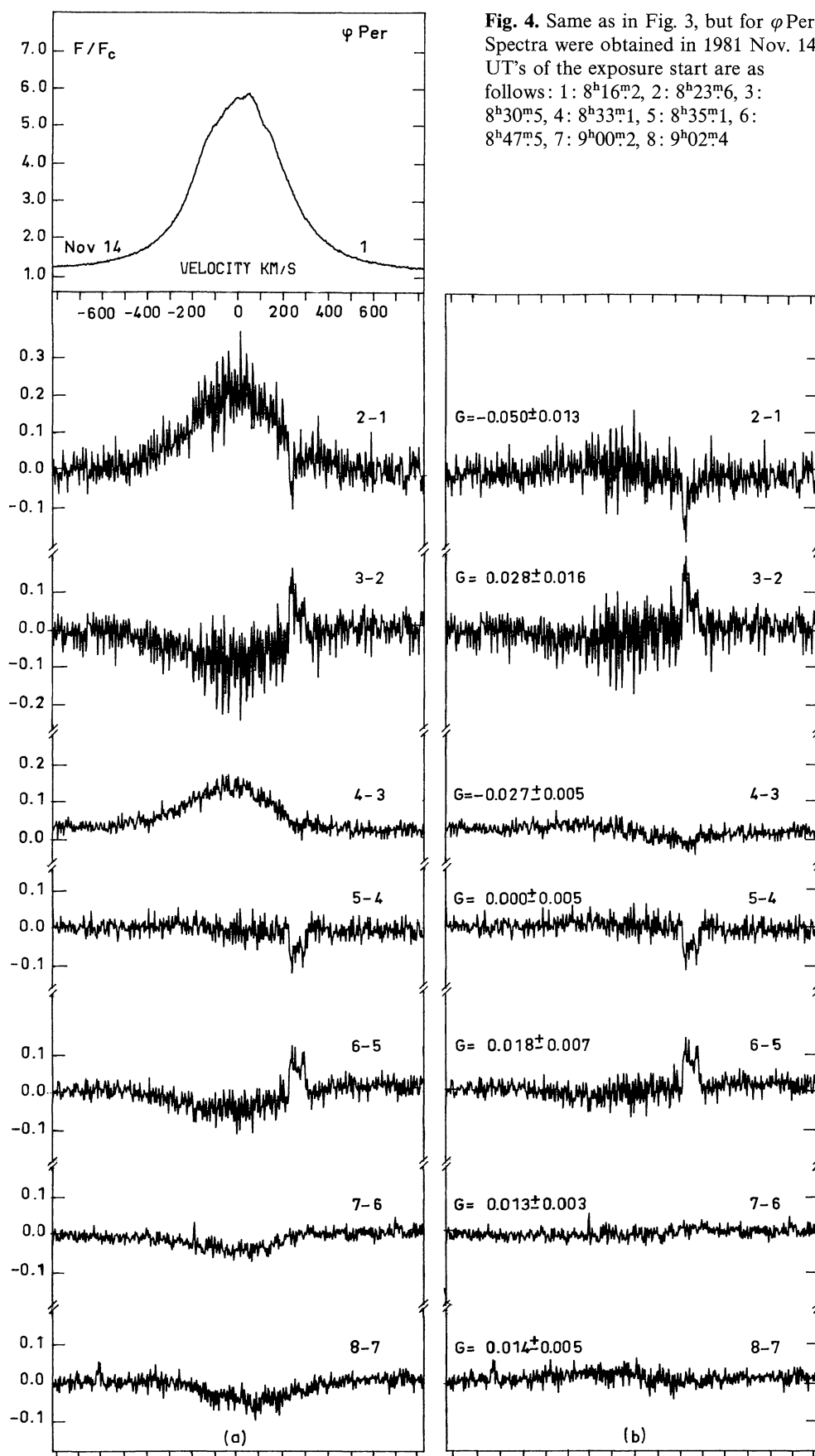
$$R'_\lambda \rightarrow R''_\lambda = 1 + \frac{R'_\lambda - 1}{1 + G_\lambda} \quad (7)$$

Indeed, in this case for the new difference of two spectra one obtains the following expression:

$$\Delta R''_\lambda = R''_\lambda - R_\lambda = \frac{L_\lambda}{F_c} \cdot \frac{G_\lambda - \bar{G}}{1 + \bar{G}} \quad (8)$$

which immediately shows that if $G_\lambda = \bar{G}$, then $\Delta R''_\lambda = 0$, and the variations due to ΔF_c are suppressed. On the other hand, at the wavelengths where the spectra have true line profile variations, $\Delta L_\lambda \neq 0$, the difference of two spectra will be:

$$\Delta R''_\lambda = \frac{L_\lambda}{F_c} \cdot \frac{\Delta L_\lambda}{L_\lambda} \cdot \frac{1}{1 + \bar{G}} \quad (9)$$



and since $\bar{G} \ll 1$, the induced modification of the line profile variations is negligible.

All differences between consecutive spectra, for which $\Delta F_c \neq 0$, were corrected by this method. The resulting plots are shown in Fig. 3b and 4b. The value of \bar{G} , calculated by means of the expression (5), and its rms deviation are indicated near the corresponding plots.

c) Instrumental origin of the continuum level variations

The values of $\Delta F_c/F_c$, calculated by means of the value \bar{G} , are sometimes significantly greater than what should be expected from the S/N ratio measured on the continuum. The reason is the presence of instrumental effects, which displaced the position of the continuum level from one spectrum to another. The effects of guiding without image slicer are responsible for the large variations $\Delta F_c/F_c$ for two sequences on November 14, as it was mentioned. Another source of such variations is the residual effect of the Reticon. By recording consecutive spectra, if there is any residue of the previously recorded spectrum stored on the Reticon pixels, the next one will be slightly modified. Special cautions to prevent this effect were taken only for observations of 59 Cyg, which are free from any instrumental effect. Nevertheless, both the residual effect and the guiding errors do not induce any small wavelength scale line profile distortions. Weak lines, such as Fe II $\lambda 6516 \text{ \AA}$ or the lines on $\lambda 8500 \text{ \AA}$ region, are not affected by the instrumental effects.

IV. Results

a) Rapid variations in H_α

No variations of the line profile are seen on the corrected difference plots for γ Cas, the upper rms limit being about 1% of the continuum flux F_c . The only variations were found for the sequence of spectra of ϕ Per, obtained in November 14 (see Fig. 4). The amplitude of the variations is 5% of the relative flux F_λ/F_c on those wavelengths. The spectra obtained in November 15 and 16 do not show any variations, the upper rms limit being 3% of F_c . No variations were found for 59 Cyg (1% of F_c).

b) Hour and night-to-night variations

In Figs. 5 and 6 we plotted spectra of γ Cas, obtained on several hours interval, and the corresponding differences. The amplitude of the variations, seen in Fig. 5, does not exceed the 3σ level, the rms uncertainty being 2% of F_c . The variations, seen in Fig. 6, run into the same amplitude, but they show a large wavelength scale pattern, and therefore a possibility that these variations have a stellar origin cannot be excluded. In Fig. 7 (γ Cas) and Fig. 8 (ϕ Per) we plotted spectra obtained on a 24 h interval. Significant changes of H_α are clearly seen.

c) Variability in $\lambda 8500 \text{ \AA}$ region

During the 15 min monitoring of γ Cas and the 30-min monitoring of ϕ Per the EW values remained constant within the accuracy of observations (see Table 2). No variations of the line profiles were detected with the upper rms limit about 1% of F_c for γ Cas and 1.5% for ϕ Per.

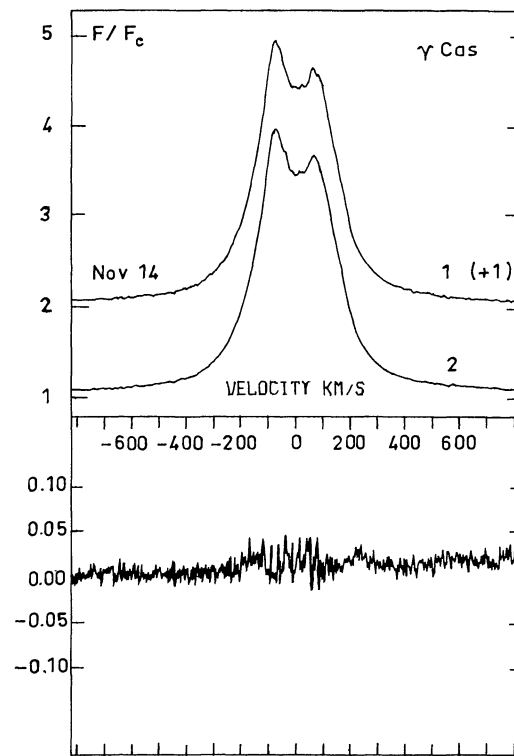


Fig. 5. Variations of the H_α line profile of γ Cas during one night. Spectra were obtained in 1981 Nov. 14, UT's are as follows: 1: $6^{\text{h}}08^{\text{m}}$; 2: $10^{\text{h}}55^{\text{m}}$. Value of a constant added to the spectrum plot is indicated in brackets

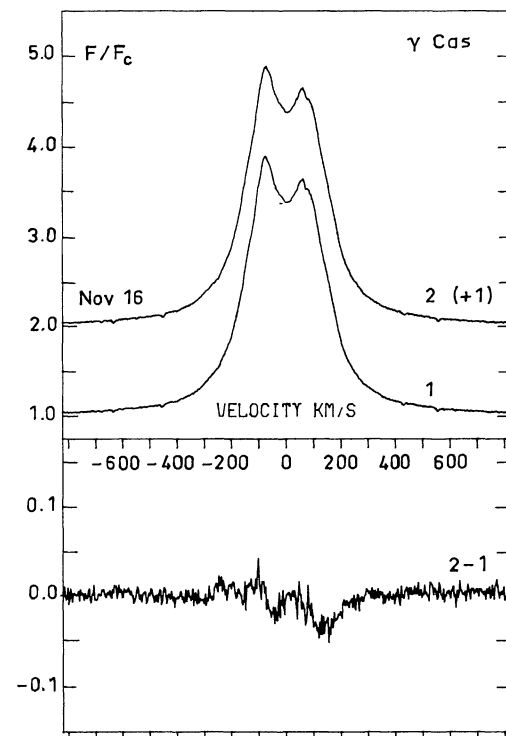


Fig. 6. Same as in Fig. 5. Spectra were obtained in 1981 Nov. 16, UT's are as follows: 1: $6^{\text{h}}03^{\text{m}}$; 2: $8^{\text{h}}22^{\text{m}}$

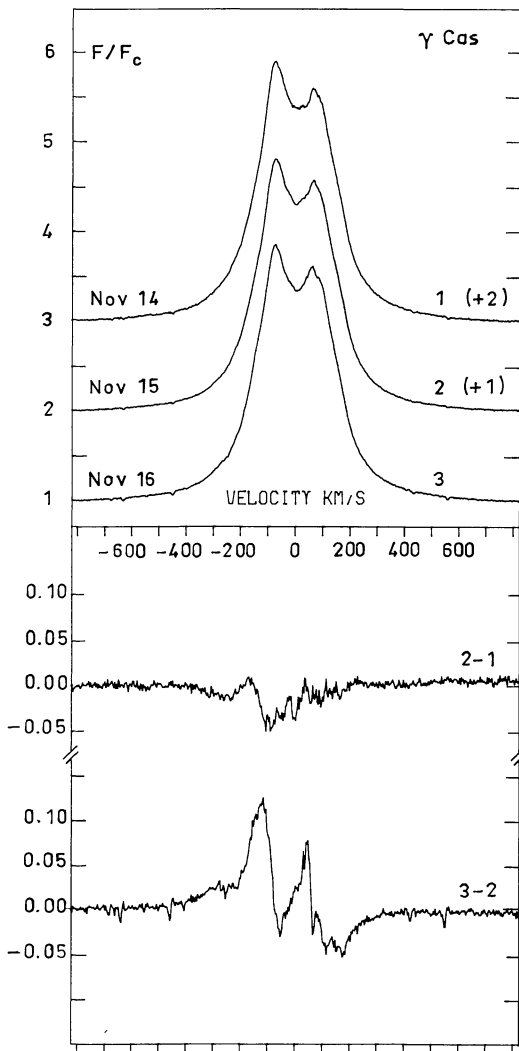


Fig. 7. Night-to-night variations of the H_α line profile of γ Cas. Spectra were obtained in the following UT's: 1: 1981 Nov. 14 6^h08^m; 2: 1981 Nov. 15 5^h47^m; 3: 1981 Nov. 16 6^h03^m

V. Discussion

γ Cas

During one night this star possibly shows slow variations of the H_α profile on a several hours scale (see Fig. 7), just at the limit of detection. If real, these variations could be consistent with the detected night-to-night distortions of the line. Both variations are caused most plausibly by the rotation of the inhomogeneous envelope. Another night-to-night variation is possibly indicated by the changes of EW of the $\text{Fe II } \lambda 6516 \text{ \AA}$. Its mean value for Nov. 16 is different from those for two other nights. If this variation is a statistically significant one, it can be explained by variations of the continuum flux at this period.

ϕ Per

Rapid variations of the H_α profile occurred on Nov. 14 for the short period of UT 8:16–8:48 (see Fig. 4). These variations differ from the “S-like” ones, described by Hutchings et al. (1971). If one continues the “letterlike” classification, then our case corresponds

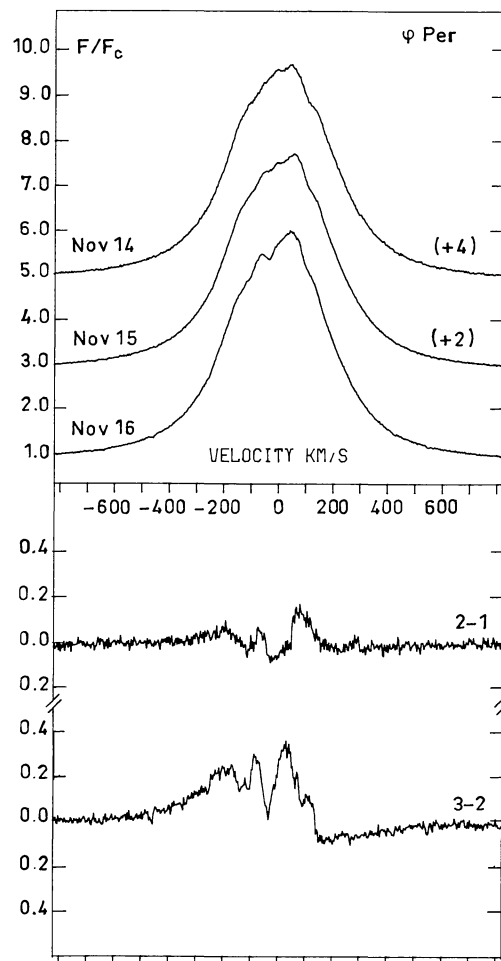


Fig. 8. Same as in Fig. 7, but for ϕ Per. Spectra were obtained in the following UT's: 1: 1981 Nov. 14 8^h16^m; 2: 1981 Nov. 15 6^h18^m; 3: 1981 Nov. 16 6^h37^m

to “U-like” variations: the changes of F_λ/F_c occur within the same small spectral interval, corresponding to $\Delta v_r \approx 100 \text{ km s}^{-1}$ and they have the same sign over all wavelengths.¹ In Fig. 9 we plotted the relative flux F_λ/F_c as a function of time. The value of F_λ/F_c for the first spectrum at UT 8:16 was taken to be 100%. One sees that the phenomenon can be described as two sequential attenuations of the light, after which the level of F_λ/F_c returns to its previous value. We can only speculate on the nature of this phenomenon. For example, one can exemplify such attenuations by a moving body, which crosses the envelope and obscures consequently 2 bright regions emitting on these wavelengths of H_α . A modified version of this hypothesis consists in two bodies crossing one bright region. Local variations of the source function are also possible to imagine. However, the obtained data supply only a little fraction of a necessary information and any reasonable conclusion is not possible. Due to the short duration and their peculiar form it seems that these variations do not represent a typical phenomenon.

¹ Malfunctions of Reticon pixels, which could be responsible for such variations, have never been detected, and an instrumental origin is excluded

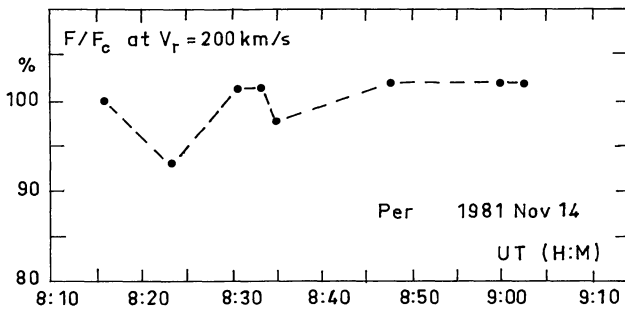


Fig. 9. Relative spectral flux of the line of ϕ Per at $V_r = 200 \text{ km s}^{-1}$ as a function of time

Possible variations of the continuum

In Sect. III we described a method to suppress variations due to the change of F_c and it was shown that in our case those variations were spurious ones. If one excludes the instrumental causes, the same method can be used to measure accurately relative variations of the stellar continuum flux, their amplitude being provided by \bar{G} . A precision about 0.5% can be achieved. The necessary condition of the method is a presence of a strong emission line, which plays the role of the comparison “object”. A search of the rapid variations of the continuum emission seems to be particularly interesting. Such variations may be caused by density inhomogeneities in the stellar wind, so that the amount of plasma, injected in the envelope, will be variable. The arising variations of the bound-bound emission will be smoothed due to a large optical thickness of the envelope, while the variations of the free-free and free-bound emissions will not be affected by transfer effects, since the envelope is optically thin in the Paschen continuum. The negative result, reported by Percy (1982) for the rapid variations of the continuum flux of γ Cas, refers to $\lambda 4670 \text{ \AA}$, where the contribution of the envelope emission is small: about 5% according to Poeckert and Marlborough (1978a). The most suitable spectral region for such a study is located near the blue side of the Paschen discontinuity, $\lambda 8204 \text{ \AA}$, where the contribution of the envelope emission becomes about 16% of the total flux according to Poeckert and Marlborough (1978), or about 50% according to Scargle et al. (1978), both models being for γ Cas. An accurate photometry of this region, carried out simultaneously with spectroscopic observations of UV-lines (Si IV, C IV, Mg II), could provide an information on the degree of homogeneity of stellar winds.

VI. Conclusions

The presented results show that in a small time scale (2–15 min) the spectra of the studied Be stars in H_α and $\lambda 8500 \text{ \AA}$ region are, in general, stable: no profile variations were found, except two brief attenuation events on H_α spectra of ϕ Per. Slow (several hours scale) distortions of the H_α line profile due, most likely, to effects of rotation of the envelope can occur, being at the limit of detection. The night-to-night changes of H_α are shown to exist. The high spectral resolution, 0.2 \AA , a good sensibility to changes of the line profile, 1–2% of F_c , accompanied by the detailed analysis of the instrumental uncertainties, make these conclusions unambiguous. This is the first high resolution study, which gives a negative result on the rapid variability in Be stars. Some doubts arise upon previous reports on the variability (instrumental effects not well retrieved). The amplitude of the profile variations found by Luud (1978) for γ Cas and by Hutchings et al. (1971) for k Dra exceeds

many times our detection limit. The arising contradiction is possibly explained by the fact that those authors used a TV-detection technique, while our spectra were obtained by a Reticon, which is more precise and more stable as a detector. Another explanation, which cannot be yet rejected, consists in assuming that the rapid profile variations are present in spectra of Be stars only during isolated short periods of activity. More similar observations of Be stars are needed to get a final definite statement.

Acknowledgements. The authors are grateful to Dr. F. Praderie, who made many constructive remarks and contributed significantly to improve this paper. We are grateful also to Drs. P. Felenbok, F. and M. Spite, A. M. Delplace-Hubert, V. Doazan, and R. Cayrel for fruitful discussions.

Appendix

The equivalent width of a line is calculated as a function of some measured quantities, which are subject to statistical fluctuations. Let us obtain an expression, which relates the uncertainty of EW to the standard deviations of its arguments, these deviations being easily measurable.

By definition,

$$W = \int_{\lambda_1}^{\lambda_2} \frac{F_c - F_\lambda}{F_c} \cdot d\lambda, \quad (\text{A1})$$

where F_c is the continuum spectral flux, F_λ is the spectral flux on the wavelengths of the spectral line, and the line occupies an interval $\lambda_1 < \lambda < \lambda_2$, so that $F_\lambda = F_c$ for $\lambda \geq \lambda_2$ and $\lambda \leq \lambda_1$.

In practice, the integral is replaced by a numerical quadrature formula. In the case of a trapezium formula applied to a normalized spectrum, one will have:

$$W = h_\lambda \cdot \sum_{j=2}^{M-1} \left[1 - \left(\frac{F_j}{F_c} \right) \right], \quad (\text{A2})$$

where h_λ is the spectral dispersion per pixel, M is the number of pixels corresponding to the interval $\lambda_1 \leq \lambda \leq \lambda_2$, and (F_j/F_c) is the relative spectral flux as measured on pixel j of the spectral line; the index $j=1$ corresponds to $\lambda = \lambda_1$. Since $F_j = F_c$ for $j=1$ and $j=M$, the corresponding terms of the sum (A2) are in mean equal to zero.

The expression (A2) provides an explicit form of the function W of the random quantities F_1, F_2, \dots, F_M and F_c . It is important that the statistical fluctuations of F_j and F_c can be considered as independent ones. Then, if those fluctuations are small, one can write:

$$W \equiv W(F_1, \dots, F_M, F_c) \simeq W(\bar{F}_1, \dots, \bar{F}_M, \bar{F}_c) + \sum_{j=1}^M \left. \frac{\partial W}{\partial F_j} \right|_{\bar{F}_j} \cdot (\bar{F}_j - F_j) + \left. \frac{\partial W}{\partial F_c} \right|_{\bar{F}_c} \cdot (\bar{F}_c - F_c). \quad (\text{A3})$$

This expression describes a function, which is linear with respect to its arguments. The standard deviation of such a function relates to those of its arguments in the following way:

$$\sigma_T^2(W) = \sum_{j=1}^M \left[\left. \frac{\partial W}{\partial F_j} \right|_{\bar{F}_j} \cdot \sigma(F_j) \right]^2 + \left[\left. \frac{\partial W}{\partial F_c} \right|_{\bar{F}_c} \cdot \sigma(F_c) \right]^2. \quad (\text{A4})$$

Using the expression (A2), the derivatives may be expressed as follows:

$$\left. \frac{\partial W}{\partial F_j} \right|_{\bar{F}_j} = - \frac{h_\lambda}{F_c}, \quad (\text{A5})$$

$$\left. \frac{\partial W}{\partial F_c} \right|_{\bar{F}_c} = \frac{1}{\bar{F}_c} (\Delta\lambda - W), \quad (\text{A6})$$

where $\Delta\lambda = \lambda_1 - \lambda_2$.

Since in our case the photon noise is negligible, we can write:

$$\sigma(F_j) = \frac{F_j}{S/N}, \quad (\text{A7})$$

where S/N is the signal-to-noise ratio measured on the continuum pixels.

Now, using relations (A5)–(A7), the expression (A4) can be rewritten in the following form:

$$\sigma_T^2(W) = \left(\frac{h_\lambda}{S/N} \right)^2 \cdot \sum_{j=1}^M \left(\frac{F_j}{\bar{F}_c} \right)^2 + \left[\frac{\sigma(\bar{F}_c)}{\bar{F}_c} (\Delta\lambda - W) \right]^2. \quad (\text{A8})$$

Now, all quantities of the right side are measurable ones, i.e. the expression (A8) provides a mean to estimate the uncertainty of a EW measurement. The value (S/N) characterizes the spread of read-outs on the continuum of an individual spectrum, while the quantity $\sigma(\bar{F}_c)$ is the total uncertainty of the continuum level determination, and these two quantities may be related by a non-simple way. For wide lines in emission, $W < 0$, the contribution of the second term of (A8) can be very important, even if $\sigma(\bar{F}_c)$ is small. For example, for our typical spectrum of γ Cas we obtain for the first term $\sigma_1(W) \ll 0.02 \text{ \AA}$, and for the second term $\sigma_2(W) \approx 0.23 \text{ \AA}$, while the value of $\sigma(\bar{F}_c)/\bar{F}_c$ is as small as 0.25%.

For practical calculations one can simplify the sum, entering in the first term of the expression (A8). In fact, one can always find such value (\tilde{F}_j/F_c) , that

$$\left(\frac{\tilde{F}_j}{\bar{F}_c} \right)^2 = \frac{1}{M} \sum_{j=1}^M \left(\frac{F_j}{F_c} \right)^2$$

and then

$$\sigma_T^2(W) = M \cdot \left(\frac{h_\lambda}{S/N} \right)^2 \cdot \left(\frac{\tilde{F}_j}{\bar{F}_c} \right)^2 + \left[\frac{\sigma(\bar{F}_c)}{\bar{F}_c} (\Delta\lambda - W) \right]^2. \quad (\text{A9})$$

Also, using the inequality:

$$\sum_{j=1}^M \left(\frac{F_j}{\bar{F}_c} \right)^2 \leq M \cdot \left(\frac{F_{j\max}}{F_c} \right)^2$$

one can estimate the upper bound for $\sigma_T(W)$ by means of the following expression:

$$\sigma_T^2(W) \leq M \cdot \left(\frac{h_\lambda}{S/N} \right)^2 \cdot \left(\frac{F_{j\max}}{F_c} \right)^2 + \left[\frac{\sigma(\bar{F}_c)}{\bar{F}_c} (\Delta\lambda - W) \right]^2.$$

A similar analysis can be developed for the case, where the photon noise is dominating, i.e.

$$\sigma(F_j) = \left(\frac{F_j}{\bar{F}_c} \right)^{1/2} \cdot \frac{\bar{F}_c}{S/N}$$

Note added in proof: We just received a paper reporting identical observations made in August 1982 of H_α for two Be stars by using the same instrumentation (Fontaine et al.: 1983, *Astron. J.* **88**, 527). The authors did not detect any very rapid variations of the line profile which supports the validity of our conclusions. However, their data call for two comments: i) The profile of H_α obtained by Fontaine et al. for γ Cas shows an important change of the V/R ratio respect to our observations in November 1981. ii) The division of spectra, method of comparison used by those authors, is less sensitive to detect line variations than the subtraction of consecutive spectra. In fact:

$$\frac{R'_\lambda}{R_\lambda} \approx 1 + \frac{L_\lambda}{L_\lambda + F_c} \left(\frac{\Delta L_\lambda}{L_\lambda} - \frac{\Delta F_c}{F_c} \right),$$

where the meaning of symbols is given in Sect. III except R'_λ which here relates to an average spectrum. Comparison with our expression (3) yields the factor $(L_\lambda + F_c)/F_c$ to convert the precision indicated by Fontaine et al. into values relative to F_c . For γ Cas this factor is about 4 and one has 2% in the case of division of spectra compared to 1% in our paper.

and then the expression (A8) can be written as follows:

$$\sigma_T^2(W) = M \cdot \left(\frac{h_\lambda}{S/N} \right)^2 \cdot \frac{\bar{F}_j}{\bar{F}_c} + \left[\frac{\sigma(\bar{F}_c)}{\bar{F}_c} (\Delta\lambda - W) \right]^2, \quad (\text{A10})$$

where

$$\frac{\bar{F}_j}{\bar{F}_c} = \frac{1}{M} \sum_{j=1}^M \frac{F_j}{F_c}.$$

References

- Baliunas, S.L., Güinan, E.F.: 1976, *Publ. Astron. Soc. Pacific* **88**, 10
 Bijaoui, A., Doazan, V.: 1979, *Astron. Astrophys.* **73**, 285
 Fontaine, G., Villeneuve, B., Landstreet, J.D., Taylor, R.H.: 1982, *Astrophys. J. Suppl.* **49**, 259
 Haefner, R., Metz, K., Schoembs, R.: 1975, *Astron. Astrophys.* **38**, 203
 Hobbs, L.M., Campbell, B.: 1982, *Astrophys. J.* **254**, 108
 Hubert-Delplace, A.M., Hubert, H.: 1979, *An Atlas of Be Stars*, Paris, Observatoire de Meudon
 Hutchings, J.B.: 1976, in *Be and Shell Stars*, Proc. IAU Symp. **70**, ed. A. Slettebak, p. 13
 Hutchings, J.B., Auman, J.R., Gower, A.S., Walker, G.A.H.: 1971, *Astrophys. J.* **170**, L 173
 Jaschek, M., Hubert-Delplace, A.M., Hubert, H., Jaschek, C.: 1980, *Astron. Astrophys. Suppl.* **42**, 103
 Lacy, C.H.: 1977, *Astrophys. J.* **212**, 132
 Lester, D.F.: 1975, *Publ. Astron. Soc. Pacific* **87**, 177
 Luud, L.: 1978, *Pis'ma v Astron. Zhurnal* **4**, 454
 Mamatkazin, A.V.: 1978, *Trudy Astrofiz. Inst. Alma-Ata (USSR)* **31**, 73
 Percy, J.R.: 1982, IAU working group on Be stars, Proc. IAU General Assembly in Patras, Greece
 Percy, J.R., Jakate, S.M., Matthews, J.M.: 1981, *Astron. J.* **86**, 53
 Poeckert, R., Marlborough, J.M.: 1978, *Astrophys. J.* **220**, 940
 Poeckert, R.: 1978b, *Astrophys. J. Suppl.* **38**, 229
 Polidan, R.S., Peters, G.J.: 1976, in *Be and Shell Stars*, Proc. IAU Symp. **70**, ed. A. Slettebak, p. 59
 Reynolds, R.C., Slettebak, A.: 1980, *Publ. Astron. Soc. Pacific* **92**, 472
 Scargle, J.D., Erickson, E.F., Witteborn, F.C., Strecker, D.W.: 1978, *Astrophys. J.* **224**, 527
 Slettebak, A.: 1979, *Space Sci. Rev.* **23**, 541
 Slettebak, A.: 1982, in *Be Stars Proc. IAU Symp.* **98**, eds. M. Jaschek and H. G. Groth, p. 109
 Slettebak, A., Snow, T.P.: 1978, *Astrophys. J.* **224**, L 127
 Slettebak, A., Reynolds, R.C.: 1978, *Astrophys. J. Suppl.* **38**, 205
 Spear, G.G., Mills, J., Snedden, S.A.: 1981, *Publ. Astron. Soc. Pacific* **93**, 460
 Underhill, A., Doazan, V.: 1982, B stars with and without emission lines, NASA SP-456